ORIGINAL PAPER

Superficial Modulus, Water-Content, and Mesh-Size at Hydrogel Surfaces

Diego I. Pedro[1] · **Duy T. Nguyen**[1] · **Lucca Trachsel**[1] · **Jose G. Rosa**[1] · **Britney Chu**[1] · **Stephen Eikenberry**[3] · **Brent S. Sumerlin**[2] · **W. Gregory Sawyer**[1]

Abstract

The most distal surfaces of lubricious high water-content aqueous gels may have decreasing concentrations and gradients of macromolecular chains on the surface that emanate outward into the environment. This superficial zone of extended polymer chains has a water-content that approaches 100% over the final few hundred nanometers, and the superficial modulus is the elastic modulus of this superficial surface. Micro-rheology using high-speed microscopy with fluorescent nanospheres enabled measurements of both the storage modulus G' and the loss modulus G'' over a frequency range of 0.4 1/s–50 1/s. 100 μm-thick control samples of polyacrylamide gels with equilibrium water-content of 97.9%, 98.4%, and 98.9% had measured storage moduli of 70.3 ± 26.9 Pa, 53.3 ± 22.4 Pa, and 38.8 ± 14 Pa, respectively. Master curves based on meta-data analysis from published measurements of mesh-size, water-content, and elastic modulus were created and used to relate rheological measurements of the superficial modulus to water-content and mesh-size. This interfacial microrheological measurement method was further used to quantify the superficial modulus and water-content of two commercial contact lens materials that have water-gradient gels on their surfaces: delefilcon A ($E = 48 \pm 11$ Pa, > 99.6% water) and lehfilcon A ($E = 10 \pm 8$ Pa, > 99.7% water). The micro-rheology method on Gemini gel interfaces facilitates measurements of the most distal superficial zone of aqueous gels and the quantification of the superficial modulus and water-content of these surfaces.

Graphic Abstract
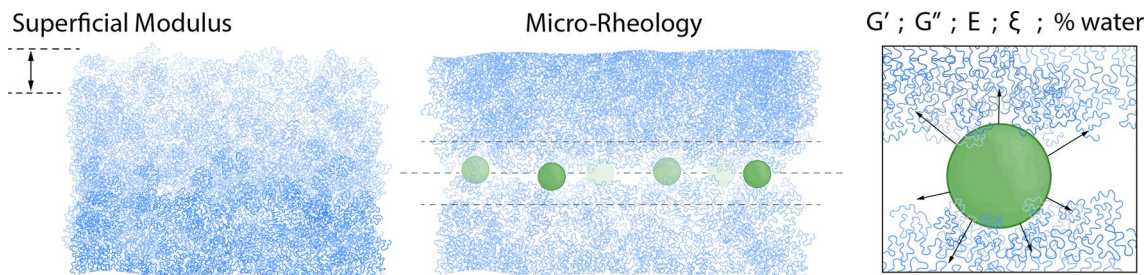
1 Introduction

The surface of many biological materials and some high water-content hydrogels have varying concentrations and gradients of macromolecular chains on the surface that emanate outward into the environment. The lubricity of hydrogels has been shown to improve by increasing the amount of water at the surface [1–5]. The superficial modulus is a suggested term to describe the effective elastic modulus of the most distal surface polymer chains of these aqueous

✉ W. Gregory Sawyer
  wgsawyer@ufl.edu

1   Department of Mechanical and Aerospace Engineering, University of Florida, Gainesville, FL 32611, USA

2   Department of Chemistry, University of Florida, Gainesville, FL 32611, USA

3   Department of Astronomy, University of Florida, Gainesville, FL 32611, USA

gels, which may be only a few hundred nanometers in thickness. The contacting surfaces of the cornea and cartilage are both covered in brushy glycosylated structures that trap large amounts of water [6]. The lubricity of aqueous gels has been linked to mesh size [5], with increasing mesh size, ξ, leading to increased water-content and decreased modulus, E. In these systems the modulus scales as $E \propto \xi^{-3}$, friction coefficient scales as $\mu \propto \xi^{-1}$, and lubricity and shear stress in Gemini gel contacts scale as $\tau \propto \xi^{-3}$ [3].

The most distal superficial surface regions of hydrogels with surface gradients are highly enriched in water and have shown exceptional lubricity [7], even super-lubricity [4]. The spontaneous formation of polymer gradients on the surfaces during casting of hydrogels against polymeric molds was first reported by the group of Gong [8] and initially thought to be the result of hydrophobicity of the mold surfaces. Recently, Simic and Spencer have demonstrated that this effect is not related to hydrophobicity but rather oxygen inhibition of free radical polymerization. Simic and Spencer went on to successfully develop a method to control oxygen availability during casting to regulate the surface structure and lubricity [9]. The ability to control the most distal superficial surface regions of hydrogels by controlling surface gradients in water-content provides a route to increase lubricity, biocompatibility, and softness of biomedical devices. Contact lenses of delefilcon A and lehfilcon A both have high water-content surface gel layers that demonstrate robust lubricity against corneal epithelial cell layers ($\tau = 16 \pm 2$ Pa) and reduced damage as compared to lenses without high water-content surface gel layers [10].

Most internal and external interfaces of animals are defined by an epithelium, which comprises polarized layer of epithelial cells. For these polarized wet epithelial cells, the apical surfaces are specialized having microvilli that produce a functional glycocalyx, which extends hundreds of nanometers and acts as an anchor to establish a lubricous gel network comprised free glycans, proteoglycans, glycolipids, and glycoproteins including soluble and gel-forming mucins. All moist non-keratinizing epithelial surfaces in the body are protected by this complex surface gel network that is graded in water-content and contains a heterogeneous network of mucin glycoproteins [11]. In biotribology, the role of hydration and the use of macromolecules to hold water and provide lubricity is a shared mechanism employed by both cartilage and the epithelium; the lubricity of cartilage is attributed to the superficial structure at the sliding surfaces [12–18].

The "Superficial Surface Modulus" is the elastic modulus of the outermost surface of a material and represents the stiffness or softness of this interfacial surface. In many cases these superficial surfaces are so soft and so thin that they are essentially inaccessible to low-force direct-contact

measurements. Micro-rheology has emerged as a leading method in bioscience to measure the viscoelastic properties of high water-content gels and materials, and one of the key benefits of this technique is the ability to perform this analysis on extremely small volumes (i.e. 1–100 μl sample volumes are sufficient for this measurement). Many materials are viscoelastic, having the ability to both store and dissipate energy; the relative contributions depend on the frequency as captured by the complex shear modulus $G*(\omega)$. The micro-rheology method is based on tracking the motion of small (microscopic) particles trapped or contained within the material. The fundamental physics underpinning this approach is the movement of microscopic beads in response to thermal stochastic forces that lead to Brownian motion. The micro-rheology approach measures the motions of these microscopic beads to quantify the mean square displacement (MSD) of the beads and then relate this to the complex shear modulus. The method, first described by Mason and Weitz in 1995 [19], has shown excellent agreement between the micro-rheology and macro-rheology measurements for a wide variety of complex fluids and is widely used in the area of biophysical sciences. In this manuscript we use micro-rheology to quantify the superficial modulus of ultra-high water-content hydrogel surfaces made from flexible hydrophilic polymers.

2 Experimental Methods

2.1 Fabrication of High Water-Content Polyacrylamide Hydrogels

The hydrogels samples were prepared by synthesizing polyacrylamide networks at 3 different concentrations: 2.75 wt%, 2.50 wt% and 2.25 wt%. The acrylamide monomer was crosslinked with N,N′-methylenebisacrylamide, using ammonium persulfate as the initiator and catalyzed by a tetramethylethylenediamine (TEMED) reductant. All solutions were prepared using ultrapure water (18.2 MΩ), and the ratio of monomer to crosslinking agent was held constant at a molar ratio of 54:1. After polymerization, samples were swollen to equilibrium in ultrapure water for approximately 80 h prior to testing. The thin hydrogel films were fabricated by adding 88 μl of polymer solution on a glass micro-coverslip (22 × 40 mm—TED PELLA, INC Prod.No:260152). In order to achieve thickness of 100 μm, an additional micro-coverslip was placed on top of the solution. After complete polymerization, the top micro-coverslip ($Ra < 1$nm) was gently removed, and the sample was allowed to swell in ultrapure water. The average surface roughness of the hydrogel was less than $Ra < 10$ nm.
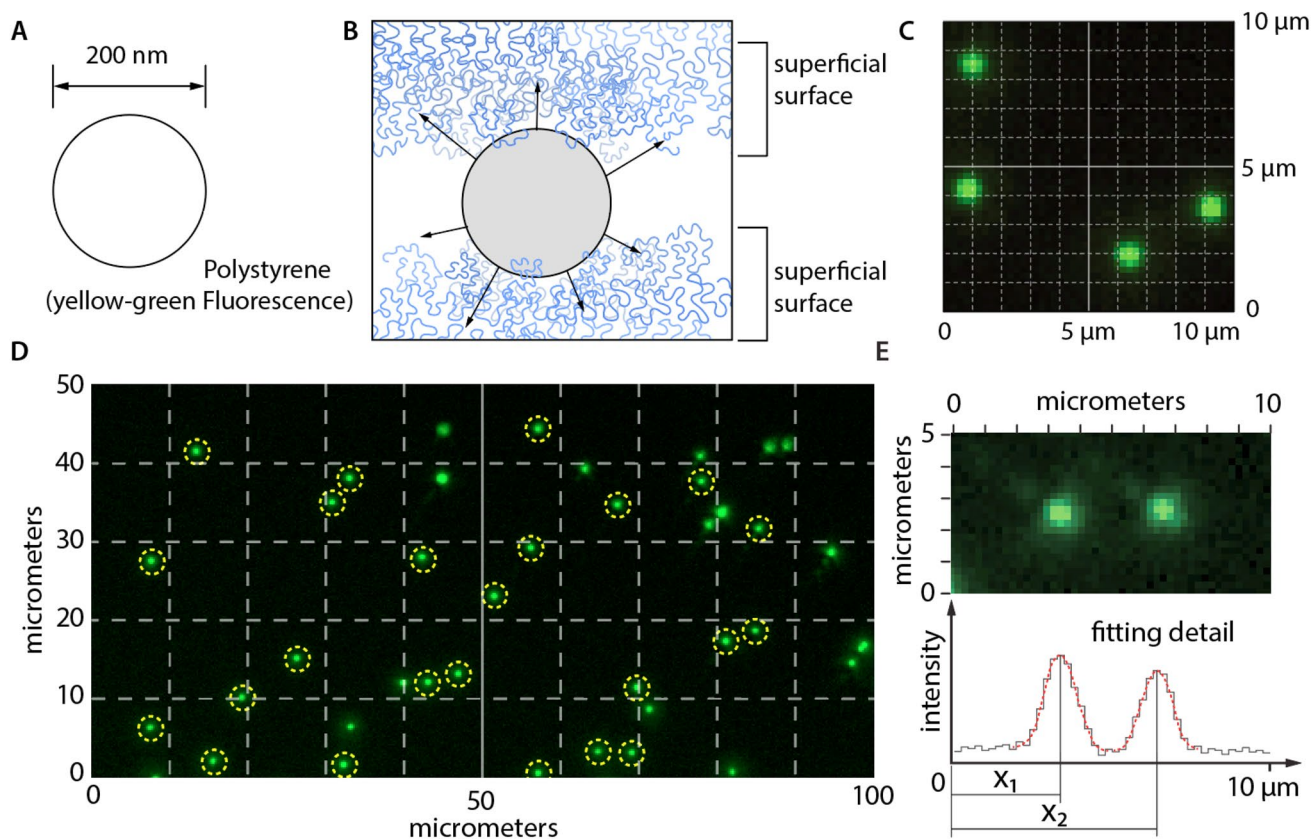
Fig. 1 A The specific beads used in these measurements were 200 nm diameter yellow-green fluorescent (505/515) FluoSpheres™ by Invitrogen™ **B** The bead movement in the superficial surface of the samples is attenuated by the mechanics of the superficial surface. **C** Images of the nanospheres are recorded using high-speed microscopy, the point spread images over a 10 μm by 10 μm subregion. **D** A representative image from experiments over an image window of 50 μm × 100 μm. The nanospheres are imaged in FITC (green) and the yellow dashed highlights indicate spheres that are in contact within the superficial surface. The positions of these nanospheres are tracked using TrackPy, and the Mean Squared Displacements (MSD) are computed from analysis of these images. **E** A zoom-in of the analysis showing image processing method, which computes a central location of the bead and then calculates the MSD by taking a differential measurement at two different time points.

2.2 Micro-Rheology and Scanning Fluorescence Confocal Microscopy

A fast laser scanning fluorescence confocal microscope (Nikon A1R) with an oil immersion Plan Apo 60X lens with a 220 μm working distance is used for imaging the motion of fluorescent nanospheres. These neutrally-buoyant polystyrene nanospheres (FluoSpheres™ by Invitrogen™) are fluorescent in yellow-green and have a reported diameter of 200 nm. An Andor iXon Ultra Back-illuminated Electron Multiplying Charge-Coupled Device (EMCCD) is used for high-speed video microscopy and captures images at 40 frames per second under FITC filtration and excitation. The aqueous gel interfaces are prepared by either mounting two identical thin films, one on top of the other, or cutting two 7 mm diameter circular samples from an identical pair of contact lens that were equilibrated in Phosphate Buffered Saline (PBS) for > 24 h.

In order to trap nanospheres within a Gemini hydrogel interface to study the superficial modulus using micro-rheology, the lower sample is placed on a glass coverslip in the optical path, a 1 μl drop with a 0.01% concentration of nanospheres is applied to the apical surface of the sample, and the second sample is then placed on top, thereby sandwiching the microsphere in the superficial zone (Fig. 1A, B) at a contact pressure below the polymer osmotic pressure [20]. The nanospheres act as a point source of light, and the point spread function leads to the pixelated image of these nanospheres as shown in Fig. 1C–E. The Brownian motion of these microspheres is captured via high-speed sequential imaging and video microscopy. Figure 1 provides a schematic illustration of the process. The thermal motion of the nanospheres trapped in the superficial surface of the aqueous gels is attenuated by the mechanics

of the interfaces, and thereby, using micro-rheology analytical techniques, can probe the rheology of this interface Fig. 1B.

Collections of images with hardware-specific time stamps were exported from the Nikon software and opened using a series of particle tracking libraries based on TrackPy, which is a widely used particle tracking software package for the biophysical sciences. The MSDs were calculated by fitting the point spread function to the images to identify central positions of the beads and subtracting the initial positions. Drift quantification and corrections were automatically implemented due to the large number of beads in the field of view. Any beads that were found to be freely moving and therefore not in contact with the surface gel layers were excluded from the analysis, as well as any agglomerated beads, which were effectively athermal.

3 Analytical Methods

3.1 Passive Micro-Rheology and Validation with Model Fluids

Following the analysis methods of Mason and Weitz [19], the average MSD as a function of lag time, τ, is given by Eq. (1).

$$\Delta r^2(\tau) = [x(t+\tau) - x(t)]^2 + [y(t+\tau) - y(t)]^2 + [z(t+\tau) - z(t)]^2 \tag{1}$$

where $\Delta r^2(\tau)$ is the average MSD; x, y, and z are coordinate positions; τ is the lag time, and t is time. For a purely viscous material, the MSD increases linearly with time. For materials that are purely elastic, the MSD will be flat, showing no dependence on time; the nanospheres will simply fluctuate around a given equilibrium position. For high water-content aqueous gels, these materials exhibit both viscous and elastic components over different timescales and require numerical methods to transform the MSD versus lag time data into viscoelastic spectra.
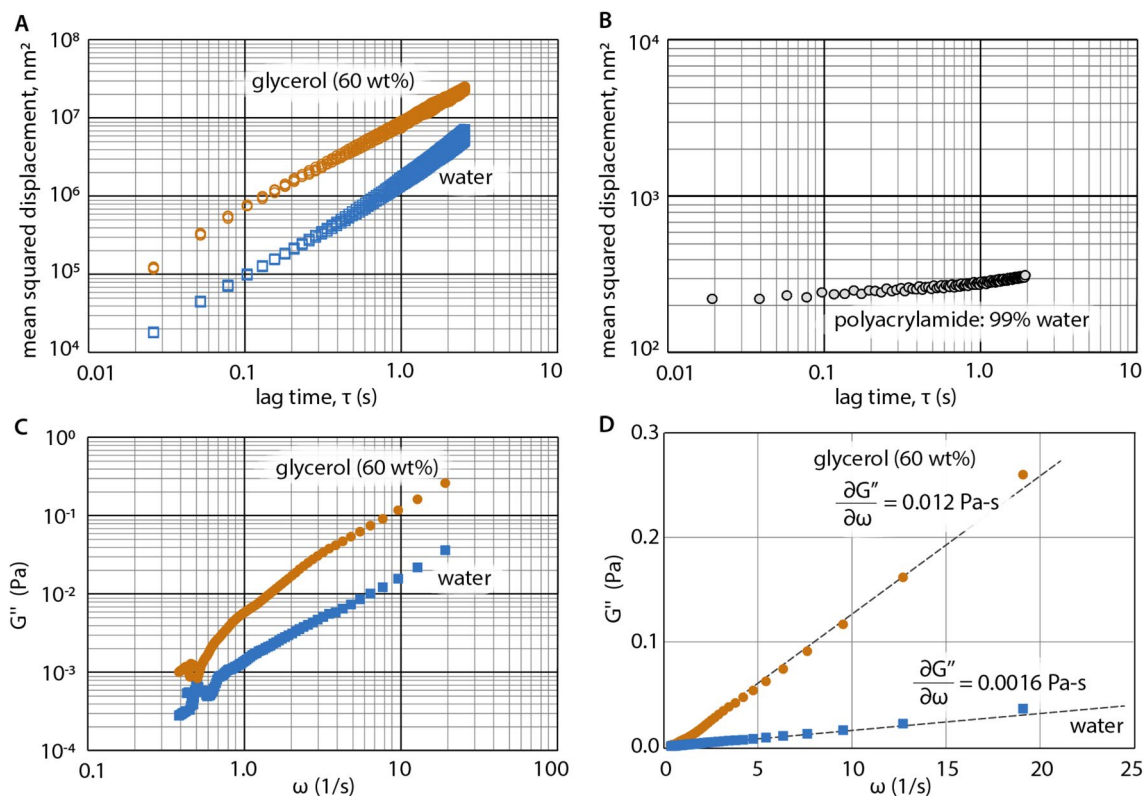

Fig. 2 A Triplicate measurements in a glycerol water solution (60 wt% glycerol and DI water; all data are shown. The glycerol data (orange) and water data (blue) show nearly linear MSD with time. **B** Representative measurement of MSD for a Gemini hydrogel interface of polyacrylamide with a water-content of 99%. **C** Analysis of the MSD of the glycerol water solution and water reveal no measurable storage modulus, G', (i.e. G'' is $> 10 \times G'$), and the frequency dependence of loss modulus, G'', is shown as a function of frequency, $\omega = 0.1$–100 1/s. **D** Demonstration of the micro-rheology approach to estimate the viscosity of these fluids.

For spherical beads embedded in a viscoelastic medium, a Generalized Stokes-Einstein Relation (GSER) can be used for complex fluids [21] with a frequency dependent viscosity; this is given by Eq. (2).

$$\tilde{G}(s) = \frac{k_B T}{\pi a s \tilde{r}^2(\tau)}. \tag{2}$$

Following the established analysis methods of micro-rheology, $\tilde{G}(s)$ is the viscoelastic spectrum as a function of the Laplace frequency, s; the particle radius is a; the thermal energy is $k_B T$; and the Laplace transform of the MSD is $\tilde{r}^2(\tau)$. The solution approach uses a local fitting of the MSD plot to a power law, which greatly simplifies the mathematics and allows straightforward frequency dependent calculations of the storage modulus, $G'(\omega)$, and the loss modulus, $G''(\omega)$. The MSD for nanospheres suspended in a 60 wt% glycerol aqueous solution and water are shown in Fig. 2A, and a representative measurement of the MSD for beads in the Gemini surface of a 99% water-content polyacrylamide sample is shown in Fig. 2B. Note that the MSD of the Gemini hydrogel interface is approximately 10^4 lower than the MSD of the model fluids.

The micro-rheology method does not involve the use of calibration constants or free parameters; rather, the application of the method to known fluids is often used to validate the micro-rheology system. Analysis of the loss modulus for the 60 wt% solution of glycerol in water and pure water is shown in Fig. 2C, D and is used to demonstrate the accuracy of the method, approach, and instrumentation. In this bead-based micro-rheology measurement, the driving force of the particle motion is thermal energy, and therefore the method is limited to measurements of soft materials and has

been widely used in biophysical sciences. Analysis of beads embedded in a transparent high-modulus material was used to evaluate instrument noise, which in turn gives a ceiling in storage modulus G' that can be accessed by the method (i.e. Brownian motions below the instrument noise cannot be quantified, and the instrument noise itself corresponds to an upper level of storage modulus, above which measurements cannot be accurately performed). For the measurements performed here, the MSD instrument noise floor has a corresponding ceiling of ~ 800 Pa in G'.

Fitting the G'' data over the range of frequencies provides an estimate of the frequency independent viscosity. As shown in Fig. 2, this recovers values consistent with the glycerol water solution and pure water, which is an extremely challenging fluid for rheological measurements. At room temperature, the aqueous glycerol solution had a measured macro-rheology viscosity of 0.011 Pa-s and a micro-rheology measured viscosity of 0.012 Pa-s; water is known to have a viscosity of ~0.001 Pa-s at room temperature.

3.2 Meta-data Analysis of the Interrelationships Between Polymer Volume Fraction, Water-Content, Mesh-Size, and Elastic Modulus

The mechanics and elasticity of aqueous gels have been carefully studied by researchers in biomedicine, chemistry, engineering, and polymer physics. A generalized framework from which to compare these studies is through the concept of polymer mesh size, ξ. Simple aqueous gels made of crosslinked polymers solvated in water have been used extensively in an effort to elucidate the relationships between the elastic modulus, polymer concentration, water-content, and mesh-size. Intercomparisons between gels of different polymers can be
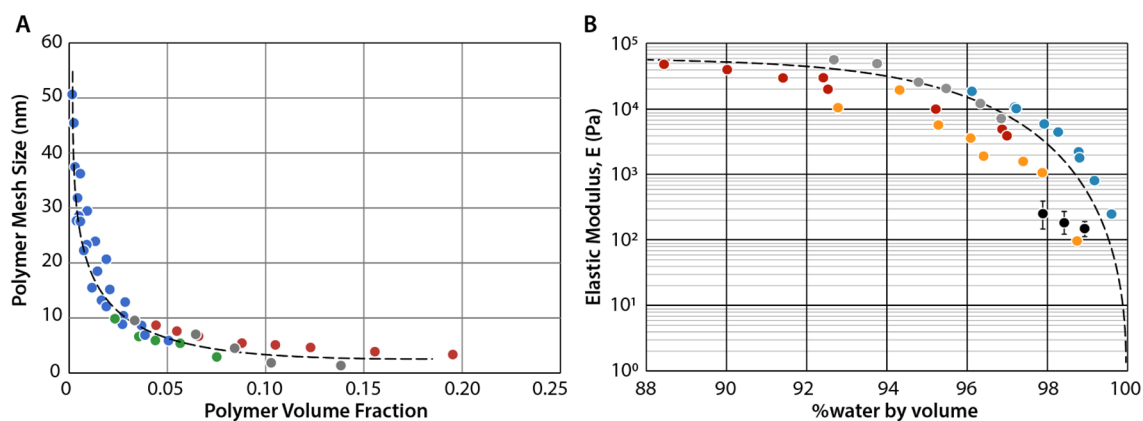

Fig. 3 Meta-data analysis of high water-content, flexible, aqueous gels of similar persistence lengths. The curve fitting of these data (dashed lines) is consistent with the scaling laws and polymer physics of hydrogels. **A** Meta-data analysis of measured mesh-size of aqueous gels in nanometers versus the polymer volume fraction by 4 different author groups showing a dramatic increase in polymer mesh size as the polymer volume fraction drops below 10%: blue [24], green [25], gray [5], and red [26]. **B** Meta-data analysis of measurements of Elastic Modulus of aqueous gels as a function of water-content: red [25], gray [27], blue [28], orange [29], and black (this study). These data show a rapid drop in the elastic modulus as the water-content increases over the range of 90–100% water.

made following considerations of the persistence length of the monomer repeat units. For the aqueous gels measured here, the analogous hydrogel materials are homogeneous, high water-content, short persistence lengths, swollen in nearly ideal solvents. The scaling concepts of polymer physics, as pioneered

Table 1 Analysis of the storage modulus of the superficial surface, G', based on the micro-rheology measurements

	$<G'>$ (Pa)	E (Pa)	Water-content (%)
Polyacrylamide	70.3 ± 26.9	211 ± 81	97.9 ± 0.1
Polyacrylamide	53.3 ± 22.4	160 ± 67	98.4 ± 0.1
Polyacrylamide	38.8 ± 14.0	116 ± 42	98.9 ± 0.1
Delefilcon A	15.9 ± 3.5	48 ± 11	$> 99.6*$
Lehfilcon A	3.3 ± 2.7	10 ± 8	$> 99.7*$

The superficial modulus E is given by $E = 3 \cdot G'$ based on the assumption of a Poisson's ratio of $\nu = 0.5$. The water contents of the polyacrylamide samples were determined directly from differential mass measurements, (*) while the delefilcon A and lehfilcon A were based on a graphical analysis of Fig. 5 after applying a coverage factor of $+ 3\sigma$.
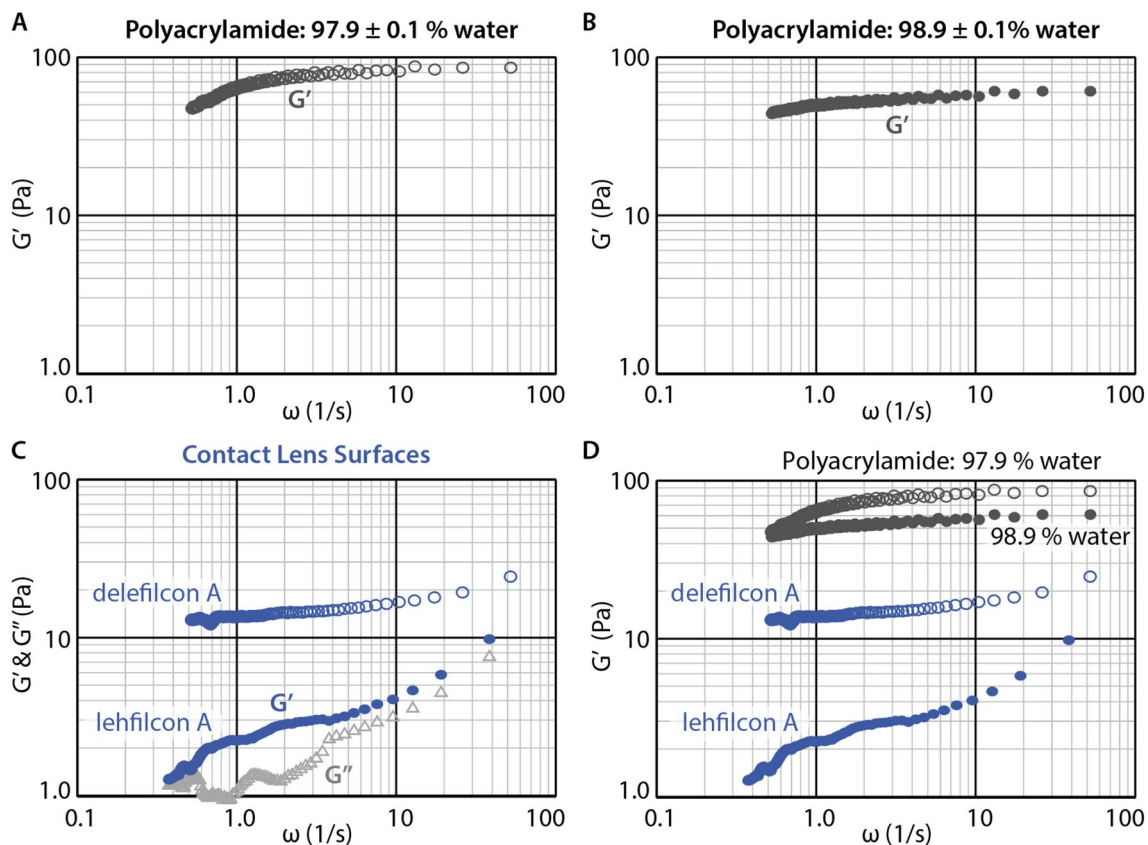
by de Gennes [22,23], have given the community a number of important relations, and generally related all mechanical and transport properties back to the polymer mesh size, ξ, thermal energy, $k_{\mathrm{B}}T$, and solvent viscosity, η. Although outstanding scaling laws, the pre-factors are generally lacking and require measurements to relate the elastic modulus and the water-content to the mesh-size directly. We have performed a meta-analysis of the available literature where two measurements were performed: either the elastic modulus and polymer volume fraction, or the mesh size and the polymer volume fraction; these data are plotted in Fig. 3 (where each color represents a unique author group).

Analysis of the curves fit to the meta-data produces the expected dependence of elastic modulus, E, to the polymer mesh size as given by Eq. (3).

$$E = \frac{k_b T}{\xi^3}. \tag{3}$$

Fig. 4 Representative micro-rheology measurements of **A** polyacrylamide: 97.9% water, **B** polyacrylamide: 98.9% water, and **C** contact lens surfaces of delefilcon A and lehfilcon A, are plotted over the frequency range of $\omega = 0.4$–50 1/s. The loss modulus, G'', of lehfilcon A is plotted in **C**, all others were insignificant. **D** Plotting the storage modulus of the superficial surface of the polyacrylamide and contact lens materials reveals that the storage modulus of the contact lens surface is significantly lower than the 98.9% water content polyacrylamide.
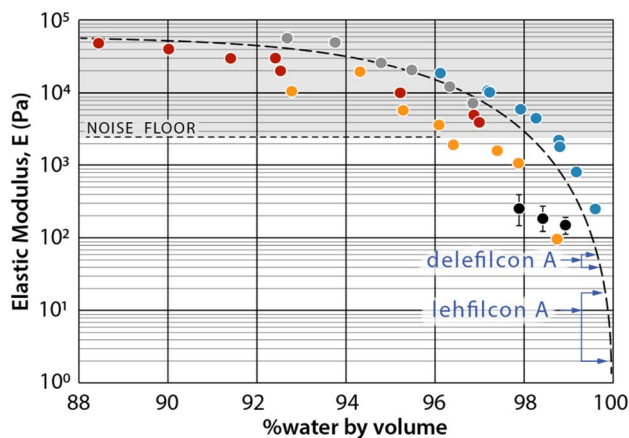
Fig. 5 Meta-data analysis and fitting of the elastic modulus versus water content (% water by volume). The MSD noise floor corresponds to a micro-rheology measurement ceiling of ~ 2400 Pa (2.4 kPa), which is indicated by a gray dashed line and highlight. The accessible micro-rheology measurement regime is indicated in white. The average measured superficial modulus of delefilcon A and Lehfilcon A are indicated by the central arrow, and the upper and lower arrows represent ± 1 standard deviation. The corresponding water content based on the superficial modulus measurements is greater than 99.6% and 99.7% for the deleficon A and lehfilcon A, respectively.

4 Results and Discussion

The three polyacrylamide control samples with five replicates each were prepared against clean glass surfaces to create hydrogel surfaces without an extended superficial zone [9]. Using differential weighing techniques following lyophilization of the prepared gels, the swollen water contents were found to be 97.9 ± 0.1%, 98.4 ± 0.1%, and 98.9 ± 0.1%. Contact lens samples of delefilcon A and lehfilcon A were also tested in the Gemini configuration to measure the superficial modulus of these contact lens materials; both of these lenses have surface gel layers with gradients in water content. Although contact lenses are curved, the long-range flexibility and the small contact spot create a planar interface that can be interrogated with this approach.

As shown in Fig. 1, each individual micro-rheology measurement involved the tracking of more than 20 beads. Each individual measurement computes an average drift corrected MSD versus lag time for the ensemble, and these measurements enable the computation of an ensemble average frequency dependent storage and loss modulus (G' and G'') over the frequency range of $\omega = 1.0$–10 s^{-1}. Four repeat measurements were made on each sample at different locations, over five different sample interfaces, and all sets were aggregated to give the mean and standard deviations provided in Table 1. Representative measurements of the superficial surface modulus for the polyacrylamide and contact lens surfaces are shown in Fig. 4. The loss modulus, G'', of the polyacrylamide samples were over tenfold below the storage modulus, G', and therefore not significant. The storage modulus decreased with increasing water content for the polyacrylamide samples.

The micro-rheology measurements on these samples reveal storage moduli that were over an order-of-magnitude lower than the noise ceiling of the experimental setup, which was determined through the analysis of imaging noise for embedded 200 nm fluorescent polystyrene nanospheres (Fig. 5). Analysis of the storage modulus over the frequency range of $\omega = 1$–10 1/s provides a mean and standard deviation for each superficial surface. Assuming a Poisson's ratio of $\nu = 0.5$, the superficial modulus can be estimated by multiplying G' by 3 (i.e. $E = 2 \cdot (1 + \nu) = 3G'$). These data, and the associated uncertainties based on the statistical analysis of the datasets, are given in Table 1, where ± represents 1 standard deviation, σ.

The superficial modulus of the polyacrylamide samples could be plotted directly on the meta-data analysis of modulus versus water content, because the water content and the superficial modulus were both directly measured (Fig. 5). The measurements of the superficial modulus of delefilcon A and lehfilcon A however do not have a direct measurement of the water content of the superficial surface. As shown in Fig. 5, the central arrow is the mean value measured for the superficial modulus, and the upper and lower arrows are ± 1σ. The water content percentages given in Table 1 for delefilcon A and lehfilcon A are based on analysis from Fig. 5, by applying a + 3σ coverage factor to these data (the results are provided in Table 1: delefilcon A > 99.6% water and lehfilcon A > 99.7% water). Taking these estimates of water content, the corresponding mesh size at the surface is on the order of 50 nm, which has a volume of less than 1.6% that of the fluorescent polystyrene nanospheres and therefore these fluorescent probes are sampling the mechanics of the superficial surface that acts as a continuum around the nanospheres.

The micro-rheology measurements provide a method to measure the superficial modulus of high water-content aqueous gels, and the meta-data analysis of high water-content aqueous gels provides a rapid method of evaluating the interrelationships between water content, modulus, and polymer mesh-size. The noise ceiling of the experimental setup can be extended into higher values using higher resolution imaging at greater magnification. The frequency range can similarly be increased using faster cameras. Overall, the current method provided direct measurements of these high water-content superficial surfaces, revealing that the surfaces of the delefilcon A and lehfilcon A have a water content greater than 99.5%.

5 Concluding Remarks

(1) Micro-rheology of Gemini hydrogel interfaces provides an opportunity for measurements of the Superficial Modulus, over distances of only a few hundred nanometers.

(2) Thin polyacrylamide gel samples were fabricated with equilibrium water contents from 97.9 to 98.9%.

(3) The meta-data analysis provides a useful and consistent graphical representation linking the polymer volume fraction, elastic modulus, water content, and mesh-size for these flexible high water-content hydrogels, such as polyacrylamide gels.

(4) Micro-rheological measurements were performed on the surfaces of a Gemini interfaces of delefilcon A and lehfilcon A contact lenses, which have a superficial modulus of 48 ± 11 Pa and 10 ± 8 Pa, respectively.

(5) Based on this analysis, the corresponding water content for the superficial surface of the delefilcon A and lehfilcon A are > 99.6% water and > 99.7% water, respectively.

Declarations

Conflict of interest The authors have no financial or proprietary interests in any material discussed in this article.

References

1. Bonyadi, S.Z., Hasan, M.M., Kim, J., Mahmood, S., Schulze, K.D., Dunn, A.C.: Review: friction and lubrication with high water content crosslinked hydrogels. Tribol. Lett. **68**, 119 (2020). https://doi.org/10.1007/s11249-020-01352-3

2. Pitenis, A.A., Urueña, J.M., Nixon, R.M., Bhattacharjee, T., Krick, B.A., Dunn, A.C., Angelini, T.E., Sawyer, W.G.: Lubricity from entangled polymer networks on hydrogels. J. Tribol. **138**, 042102 (2016). https://doi.org/10.1115/1.4032889

3. Pitenis, A.A., Sawyer, W.G.: Lubricity of high water content aqueous Gels. Tribol. Lett. **66**, 113 (2018). https://doi.org/10.1007/s11249-018-1063-5

4. Pitenis, A.A., Urueña, J.M., Cooper, A.C., Angelini, T.E., Sawyer, W.G.: Superlubricity in Gemini hydrogels. J. Tribol. **138**, 042103 (2016). https://doi.org/10.1115/1.4032890

5. Urueña, J.M., Pitenis, A.A., Nixon, R.M., Schulze, K.D., Angelini, T.E., Sawyer, W.G.: Mesh size control of polymer fluctuation lubrication in Gemini hydrogels. Biotribology **1–2**, 24–29 (2015). https://doi.org/10.1016/j.biotri.2015.03.001

6. Meier, Y.A., Zhang, K., Spencer, N.D., Simic, R.: Linking friction and surface properties of hydrogels molded against materials of different surface energies. Langmuir **35**, 15805–15812 (2019). https://doi.org/10.1021/acs.langmuir.9b01636

7. Dunn, A.C., Urueña, J.M., Huo, Y., Perry, S.S., Angelini, T.E., Sawyer, W.G.: Lubricity of surface hydrogel layers. Tribol. Lett. **49**, 371–378 (2013). https://doi.org/10.1007/s11249-012-0076-8

8. Kii, A., Xu, J., Gong, J.P., Osada, Y., Zhang, X.: Heterogeneous polymerization of hydrogels on hydrophobic substrate. J. Phys. Chem. B **105**, 4565–4571 (2001). https://doi.org/10.1021/jp003242u

9. Simič, R., Spencer, N.D.: Controlling the friction of gels by regulating interfacial oxygen during polymerization. Tribol. Lett. **69**, 86 (2021). https://doi.org/10.1007/s11249-021-01459-1

10. Hart, S.M., McGhee, E.O., Urueña, J.M., Levings, P.P., Eikenberry, S.S., Schaller, M.A., Pitenis, A.A., Sawyer, W.G.: Surface gel layers reduce shear stress and damage of corneal epithelial cells. Tribol. Lett. **68**, 106 (2020). https://doi.org/10.1007/s11249-020-01344-3

11. Linden, S.K., Sutton, P., Karlsson, N.G., Korolik, V., McGuckin, M.A.: Mucins in the mucosal barrier to infection. Mucosal Immunol. **1**, 183–197 (2008). https://doi.org/10.1038/mi.2008.5

12. Zhang, K., Simic, R., Spencer, N.D.: Imparting ultralow lubricity to double-network hydrogels by surface-initiated controlled radical polymerization under ambient conditions. Biotribology **26**, 100161 (2021). https://doi.org/10.1016/j.biotri.2021.100161

13. Seror, J., Zhu, L., Goldberg, R., Day, A.J., Klein, J.: Supramolecular synergy in the boundary lubrication of synovial joints. Nat. Commun. **6**, 6497 (2015). https://doi.org/10.1038/ncomms7497

14. Ma, L., Gaisinskaya-Kipnis, A., Kampf, N., Klein, J.: Origins of hydration lubrication. Nat. Commun. **6**, 1–6 (2015). https://doi.org/10.1038/ncomms7060

15. Lin, W., Klein, J.: Recent progress in cartilage lubrication. Adv. Mater. **33**, 2005513 (2021). https://doi.org/10.1002/adma.202005513

16. Moore, A.C., Burris, D.L.: Tribological rehydration of cartilage and its potential role in preserving joint health. Osteoarthr. Cartil. **25**, 99–107 (2017). https://doi.org/10.1016/j.joca.2016.09.018

17. Shoaib, T., Espinosa-Marzal, R.M.: Insight into the viscous and adhesive contributions to hydrogel friction. Tribol. Lett. **66**, 96 (2018). https://doi.org/10.1007/s11249-018-1045-7

18. Li, A., Ramakrishna, S.N., Kooij, E.S., Espinosa-Marzal, R.M., Spencer, N.D.: Poly(acrylamide) films at the solvent-induced glass transition: adhesion, tribology, and the influence of crosslinking. Soft Matter **8**, 9092 (2012). https://doi.org/10.1039/c2sm26222c

19. Mason, T.G., Weitz, D.A.: Optical measurements of frequency-dependent linear viscoelastic moduli of complex fluids. Phys. Rev. Lett. **74**, 1250–1253 (1995). https://doi.org/10.1103/PhysRevLett.74.1250

20. Schulze, K.D., Hart, S.M., Marshall, S.L., O'Bryan, C.S., Urueña, J.M., Pitenis, A.A., Sawyer, W.G., Angelini, T.E.: Polymer osmotic pressure in hydrogel contact mechanics. Biotribology **11**, 3–7 (2017). https://doi.org/10.1016/j.biotri.2017.03.004

21. Mason, T.G.: Estimating the viscoelastic moduli of complex fluids using the generalized Stokes-Einstein equation. Rheol. Acta **39**, 371–378 (2000). https://doi.org/10.1007/s003970000094

22. De Gennes, P.G.: Scaling Concepts in Polymer Physics. Cornell University Press, Ithaca (1979)

23. Gordon, M.: Scaling Concepts in Polymer Physics. Cornell University Press, Ithaca (1981)

24. Munoz-Pinto, D.J., Samavedi, S., Grigoryan, B., Hahn, M.S.: Impact of secondary reactive species on the apparent decoupling of poly(ethylene glycol) diacrylate hydrogel average mesh size and modulus. Polymer (Guildf). **77**, 227–238 (2015). https://doi.org/10.1016/j.polymer.2015.09.032

25. Bhattacharyya, A., O'Bryan, C., Ni, Y., Morley, C.D., Taylor, C.R., Angelini, T.E.: Hydrogel compression and polymer osmotic

pressure. Biotribology **22**, 100125 (2020). https://doi.org/10.1016/j.biotri.2020.100125

26. Park, I.H., Johnson, C.S., Gabriel, D.A.: Probe diffusion in polyacrylamide gels as observed by means of holographic relaxation methods: search for a universal equation. Macromolecules **23**, 1548–1553 (1990). https://doi.org/10.1021/ma00207a052

27. Wu, P.-J., Kabakova, I.V., Ruberti, J.W., Sherwood, J.M., Dunlop, I.E., Paterson, C., Török, P., Overby, D.R.: Water content, not stiffness, dominates Brillouin spectroscopy measurements in hydrated materials. Nat. Methods. **15**, 561–562 (2018). https://doi.org/10.1038/s41592-018-0076-1

28. Horkay, F., Magda, J., Alcoutlabi, M., Atzet, S., Zarembinski, T.: Structural, mechanical and osmotic properties of injectable hyaluronan-based composite hydrogels. Polymer (Guildf). **51**, 4424–4430 (2010). https://doi.org/10.1016/j.polymer.2010.06.027

29. Girardo, S., Träber, N., Wagner, K., Cojoc, G., Herold, C., Goswami, R., Schlüßler, R., Abuhattum, S., Taubenberger, A., Reichel, F., Mokbel, D., Herbig, M., Schürmann, M., Müller, P., Heida, T., Jacobi, A., Ulbricht, E., Thiele, J., Werner, C., Guck, J.: Standardized microgel beads as elastic cell mechanical probes. J. Mater. Chem. B **6**, 6245–6261 (2018). https://doi.org/10.1039/C8TB01421C